JACC: CARDIOVASCULAR IMAGING VOL. 6, NO. 6, 2013

ISSN 1936-878X/$36.00
PUBLISHED BY ELSEVIER INC. http://dx.doi.org/10.1016/j.jcmg.2013.04.005

iREVIEWS

STATE-OF-THE-ART PAPER

CV Imaging: What Was New in 2012?

Stephan Achenbach, MD,* Matthias G. Friedrich, MD,† Eike Nagel, MD,‡ Christopher M. Kramer, MD,§ Philip A. Kaufmann, MD,‖ Amir Farkhooy, MD,¶ Vasken Dilsizian, MD,# Frank A. Flachskampf, MD¶

Erlangen, Germany; Montreal, Quebec, Canada; London, United Kingdom; Charlottesville, Virginia; Zurich, Switzerland; Uppsala, Sweden; and Baltimore, Maryland

Echocardiography, single-photon emission computed tomography (SPECT), positron emission tomography (PET), cardiac magnetic resonance, and cardiac computed tomography can be used for anatomic and functional imaging of the heart. All 4 methods are subject to continuous improvement. Echocardiography benefits from the more widespread availability of 3-dimensional imaging, strain and strain rate analysis, and contrast applications. SPECT imaging continues to provide very valuable prognostic data, and PET imaging, on the one hand, permits quantification of coronary flow reserve, a strong prognostic predictor, and, on the other hand, can be used for molecular imaging, allowing the analysis of extremely small-scale functional alterations in the heart. Magnetic resonance is gaining increasing importance as a stress test, mainly through perfusion imaging, and continues to provide very valuable prognostic information based on late gadolinium enhancement. Magnetic resonance coronary angiography does not substantially contribute to clinical cardiology at this point in time. Computed tomography imaging of the heart mainly concentrates on the imaging of coronary artery lumen and plaque and has made substantial progress regarding outcome data. In this review, the current status of the 5 imaging techniques is illustrated by reviewing pertinent publications of the year 2012. (J Am Coll Cardiol Img 2013;6:714–34) © 2013 by the American College of Cardiology Foundation

Echocardiography

By far the most frequently applied modality of cardiac imaging, echocardiography continues to be indispensable for the practice of cardiology as well as for cardiovascular research and, despite going back 60 years since Inge Edler's initial observations, major developments continue in echocardiography. This concerns both the technique itself and its clinical and research applications. Two-dimensional echocardiography remains the "workhorse" application for assessment of cardiac morphology, dimensions, volumes, and function. Doppler echocardiography permits measurement and visualization of blood flow velocity. Derived information includes pressure

From the *Department of Cardiology, University of Erlangen, Erlangen, Germany; †Montreal Heart Institute, Cardiology, Montreal, Quebec, Canada; ‡Division of Imaging Sciences and Biomedical Engineering, King's College, London, United Kingdom; §Departments of Medicine and Radiology, University of Virginia Health System, Charlottesville, Virginia; ‖Department of Radiology, Cardiac Imaging, University Hospital Zurich, Zurich, Switzerland; ¶Uppsala Universitet, Akademiska Sjukhuset, Uppsala, Sweden; and the #Department of Diagnostic Radiology and Nuclear Medicine, University of Maryland School of Medicine, Baltimore, Maryland. Dr. Achenbach has received research grants from Siemens and Schering; and consulting fees from Guerbet. Dr. Nagel has received grant support from Philips Healthcare and Bayer Healthcare. Dr. Kramer has received research equipment support from Siemens Healthcare; and is a consultant for Synarc. All other authors have reported that they have no relationships relevant to the contents of this paper to disclose.

Manuscript received February 21, 2013; accepted April 25, 2013.

gradients, flow volumes (by combining blood flow velocity with anatomic information), and valve orifice areas. Doppler imaging is not limited to blood flow but can also be used to analyze the motion of tissue, which in turn permits applications such as imaging of myocardial deformation (strain and strain rate). Additional echocardiographic techniques include 3-dimensional echocardiography and contrast echocardiography—all areas in which major progress continues.

Morphology and function. Although echocardiography has been available for decades, even the careful analysis of cardiac morphology may produce new and relevant information. For example, noncompaction cardiomyopathy, although relatively newly recognized as a disease entity, is often overdiagnosed; no universally accepted standard of diagnosis exist. Gebhard et al. (1) introduced a new criterion for the diagnosis of this disease: the measurement of systolic compacta thickness. They found that a systolic thickness <8 mm of the compacted, outer layer of myocardium in systole (the compacta), measured in apical or mid-ventricular parasternal short-axis views, successfully separated patients with cardiomyopathy from patients with hypertrophy due to aortic valve disease. It is generally recognized that diagnosis of this disease is difficult, and overdiagnosis probably occurs frequently in individuals with some degree of hypertrophy and prominent left ventricular trabeculation.

Right ventricular assessment is more difficult than imaging of the left ventricle, given the irregular shape of the right ventricle. This concerns both morphology and function. In a study of the size of the right ventricle in endurance athletes, 28% of these individuals fulfilled the echocardiographic criteria for arrhythmogenic right ventricular cardiomyopathy (2). Hence, great caution should be used when evaluating right heart dimensions in endurance-trained persons. The authors also argued that indexing for body surface area is suboptimal to establish normal values because typically the relationship of cardiac dimensions to body surface area is not linear.

Echocardiography is the standard tool to diagnose both systolic and diastolic dysfunction of the left ventricle. For diagnosing diastolic dysfunction in patients with heart failure and preserved ejection fraction (HFPEF), the main parameters to consider are left atrial volume, the ratio of peak transmitral flow velocity to peak early diastolic left ventricular lengthening velocity (E/e′), and the transmitral diastolic flow profile. Although filling pressures cannot be measured directly by echocardiography, a reasonably reliable diagnosis of elevated left ventricular filling pressures can still be made in the majority of patients. Increased left atrial volume is already known as an essential cornerstone in the diagnosis of HFPEF. New data from the I-PRESERVE (Irbesartan in Heart Failure With Preserved Systolic Function) study in 745 patients confirm that HFPEF is associated with left ventricular hypertrophy, increased left atrial size, and other echocardiographic signs of diastolic dysfunction (3). Furthermore, these parameters significantly predict an adverse prognosis regarding mortality and heart failure–related hospitalization.

Not only increased left atrial size, but also decreased left atrial function is relevant. Russo et al. (4) showed in a community-based study of 357 patients with predominantly normal ejection fraction and in sinus rhythm that minimum left atrial volume (i.e., volume immediately after mitral valve closure) correlated better with the degree of diastolic dysfunction than maximal (systolic) left atrial volume, which is the standard measure. This might be because minimum left atrial volume, in contrast to maximum volume, contains additional information on left atrial function, which may be affected earlier by diastolic dysfunction than maximal left atrial volume. These findings are confirmed by a study by Welles et al. (5) of 855 patients with coronary artery disease and preserved ejection fraction. Left atrial function was measured by an echocardiographic index and a strong linear relationship was seen between a decrease in this index over time and adverse cardiovascular outcomes.

Echocardiography permits quantification of left ventricular stroke volumes. Analysis of stroke volume may provide complementary information in one of the most frequent disease entities studied by echocardiography, aortic valve stenosis. Lancellotti et al. (6) followed 150 asymptomatic patients with severe aortic stenosis (orifice area <1 cm^2) and normal left ventricular ejection fraction for >3 years (6). The patients were divided into 4 hemodynamically different groups depending on left ventricular stroke volume and mean pressure gradients. The study showed that patients with low stroke volume/low gradient aortic stenosis had markedly reduced cardiac event-free survival (hazard ratio [HR]: 5.4) compared with those with low stroke volume/high gradient, suggesting that integrating stroke volume

ABBREVIATIONS AND ACRONYMS

2D = 2-dimensional
3D = 3-dimensional
CI = confidence interval
CT = computed tomography
CMR = cardiovascular magnetic resonance
FFR = fractional flow reserve
FFR_{CT} = CT-derived fractional flow reserve
HFPEF = heart failure with preserved ejection fraction
HR = hazard ratio
ICD = implantable cardioverter-defibrillator
LGE = late gadolinium enhancement
OR = odds ratio
PET = positron emission tomography
SPECT = single-photon emission computed tomography
TEE = transesophageal echocardiography

JACC: CARDIOVASCULAR IMAGING, VOL. 6, NO. 6, 2013
JUNE 2013:714–34

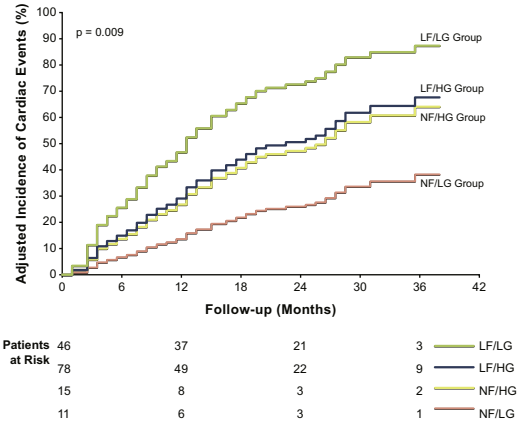

Figure 1. Adjusted Incidence of Cardiac Events According to the Newly Proposed Classification of Aortic Stenosis

HG = high gradient; LF = low flow; LG = low gradient; NF = normal flow. Reproduced, with permission, from Lancellotti et al. (6).

data allows a better prediction of clinical outcomes in patients with asymptomatic severe aortic stenosis (Fig. 1).

New insights continue to be obtained even for the assessment of cardiac morphology and function by echocardiography. Larger-than-expected right heart dimensions should be anticipated in endurance athletes, and exercise function of the right ventricle should be evaluated before concluding that a cardiomyopathy is present. HFPEF is a topic of increasing importance, and diastolic left ventricular dysfunction, left atrial enlargement, and left atrial dysfunction are closely linked.

3-dimensional echocardiography. Three-dimensional (3D) echocardiography has a proven track record for more accurate and reproducible assessment of left ventricular volumes compared with 2-dimensional (2D) imaging, even though some technical problems remain, and recalibration of "normal ranges" may be necessary (7,8). The recognition of HFPEF fraction as an important form of heart failure (see previously) has renewed interest in left atrial volumes because these are typically altered as a consequence of diastolic left ventricular dysfunction, as already discussed in the section on morphology and function. A multicenter study comparing left atrial volume calculation by transthoracic (biplane) 2D echocardiography, transthoracic 3D echocardiography, and magnetic resonance imaging as the gold standard confirmed higher accuracy and lower variability for 3D echocardiography compared with 2D echocardiography (9). This was true not only for maximal but also for minimal left atrial volumes and contributes to establishing 3D echocardiography as the best echocardiographic method to measure atrial dimensions. For the guidance of cardiac interventions, prominently mitral valve repair, 3D echocardiography has become a cornerstone (10,11).

Strain and strain rate. Doppler echocardiography can be used not only to measure blood flow velocities, but also to measure tissue velocities, such as the speed of motion of the left ventricular myocardium. However, such velocity measurements would assess the speed of motion relative to the transducer and not the deformation (e.g., shortening) of the myocardium independent from motion of the entire heart and ventricular wall. Passive motion could not be differentiated from active contraction. This limitation is overcome by strain and strain rate measurements. By comparing velocities of small myocardial segments with relative to the adjacent tissue, strain rate can be derived—the rate of shortening specific to the respective piece of myocardium, a measure of regional contractility. Strain is the integral of strain rate; it determines the overall amount of shortening in a given piece of myocardium and is a measure of regional ejection fraction (12). Strain and strain rate allow detailed and quantitative analysis of left ventricular function and can help differentiate specific disease entities. For example, in patients with amyloidosis, Phelan et al. (13) observed that apical segments seem to be mostly "spared" from impairment of longitudinal strain; this finding effectively distinguished patients with cardiac amyloidosis from those with left ventricular hypertrophy or hypertrophy due to aortic stenosis.

The detailed and quantitative analysis of myocardial contraction has been used to analyze *ischemic memory*, a loosely defined concept referring to structural or functional changes in the myocardium after a transient ischemic episode has resolved (14). Different from infarction, no permanent damage is caused by such a brief episode; however, the structural or functional changes, although ultimately reversible, last longer than impairment of perfusion and therefore metaphorically have been dubbed a memory. An example is the well-known phenomenon of myocardial stunning. In a modification of previous work by Ishii et al. (15), Asanuma et al. (16) demonstrated in an experimental animal model that after a 2-min coronary occlusion, post-systolic shortening (myocardial shortening occurring after aortic valve closure) persisted as long as 20 min after reperfusion. This could be measured preferentially by speckle tracking–based circumferential strain measurements (Fig. 2).

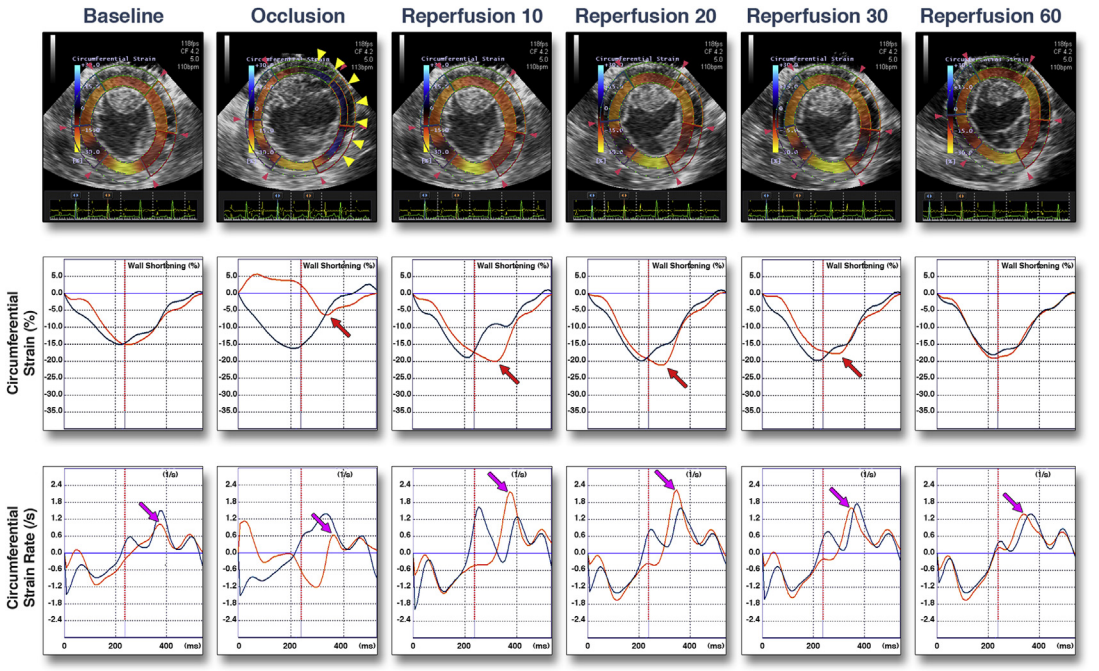

Figure 2. Strain and Strain Rate Profiles

(Top) End-systolic circumferential strain is color coded in the inner half of the myocardium. Orange color disappeared in the risk area **(yellow arrowheads**) during coronary occlusion, indicating that end-systolic strain was near 0. **(Middle)** Circumferential strain profiles in the risk area **(orange line)** and the normal area **(blue line)**. Post-systolic shortening was demonstrated in the risk area during occlusion. Although systolic strain recovered to the baseline level by 10 min after reperfusion, post-systolic shortening persisted until 30 min after reperfusion **(red arrows)**. **(Bottom)** Circumferential strain rate profiles in the risk area **(orange line)** and the normal area **(blue line)**. Strain rate during early diastole **(pink arrows)** decreased in the risk area during occlusion, but this decrease did not persist after reperfusion. End-systole is indicated by the **red dotted line**. Reprinted, with permission, from Asanuma et al. (16).

Obviously, such observations, if reliably reproducible in a clinical context, might be very useful to improve accuracy for ischemia detection at rest or after a stress test.

Another example in which strain and strain rate image may provide crucial information is the clinical problem of low-flow–low-gradient aortic valve stenosis, a situation in which the assessment of the degree of aortic valve stenosis may be very difficult. In a prospective cohort study of patients with aortic stenosis by Herrmann et al. (17), the investigators analyzed whether echocardiographic measurements could detect myocardial fibrosis, thus allowing the differentiation between low-gradient, paradoxical severe aortic stenosis with myocardial fibrosis from moderate aortic stenosis with similar gradients, but without or with less fibrosis. Myocardial fibrosis was quantified by contrast-enhanced magnetic resonance imaging. On follow-up, patients with myocardial fibrosis had poorer outcomes than those with little or no fibrosis. Echocardiographic parameters of longitudinal left ventricular function (mitral ring displacement or longitudinal strain rate) reliably identified the functional consequences and thus the presence of myocardial fibrosis (Fig. 3).

Strain and strain rate imaging can also be applied to the right ventricle. La Gerche et al. (18) analyzed right ventricular function in endurance athletes with right ventricular strain and strain rate measurements and found lower than normal values at rest, with a large increase with exercise.

Longitudinal left ventricular function may serve as an indicator of early myocardial damage, even if ejection fraction is preserved. This holds true for ischemic damage as well as early cardiomyopathy, fibrotic myocardial remodeling in aortic stenosis, and other conditions.

Contrast echocardiography. Contrast echocardiography has been used, for example, for better quantification of left ventricular function and the analysis of myocardial perfusion. As a reminder that fundamental technical improvements, although currently more sluggish than in CT or CMR, can also be expected for echocardiography, a pre-clinical

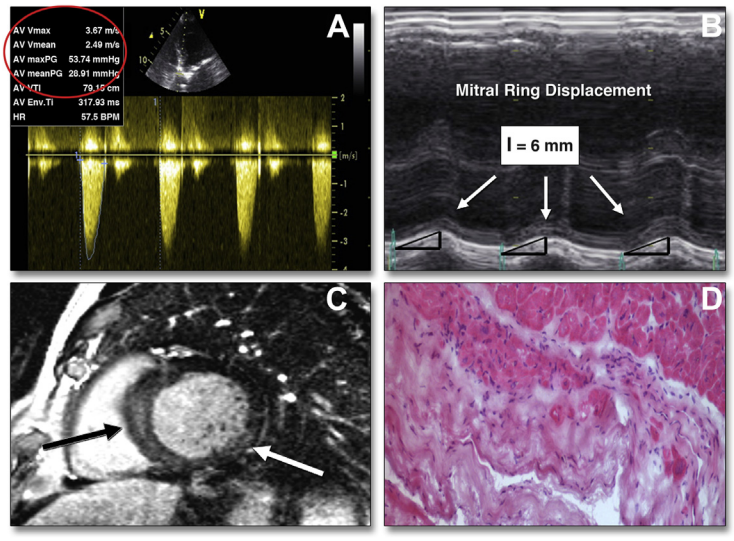

Figure 3. Patient With a Typical Pattern of Low-Gradient Aortic Stenosis

(A) A 78-year-old woman with a septal and posterior wall of 13 mm, left ventricular end-diastolic diameter of 40 mm, ejection fraction of 60%, aortic valve area of 0.9 cm^2, and mean gradient of 29 mm Hg. **(B)** Mitral ring displacement is 6 mm (normal value, <9 mm). **(C)** Typical basal septal and lateral late enhancement **(arrows)** on cardiac magnetic resonance imaging. **(D)** Marked myocardial fibrosis on histology from intraoperative biopsy. Reprinted, with permission, from Herrmann et al. (17).

report from Dave et al. (19) illustrates an ingenious use of contrast echocardiography to determine the absolute pressure level to which contrast agents are exposed, harnessing an inverse relationship between ambient pressure and reflectivity. More precisely, the amplitude of reflection from a bubble at one half of the insonation frequency is linearly and inversely related to the pressure in the fluid surrounding the bubbles, a concept called "subharmonic aided pressure estimation." After proper calibration, the researchers were able to track remarkably well the left ventricular pressure curve based on data extraction from (noninvasive) pulsed-wave Doppler recordings of the left ventricle. If robust enough, the applications of such a technique would be legion.

Nuclear Cardiology (SPECT and PET)

SPECT and PET are the major techniques used in nuclear cardiology, with SPECT being used in a substantially larger portion of patients. Myocardial perfusion imaging at rest and stress is the standard approach to identify reversible defects of tracer accumulation as a sign of exercise-induced hypoperfusion and/or fixed defects at rest and stress as a sign of myocardial scar. In addition to their diagnostic value, SPECT and PET imaging of myocardial perfusion and viability have a strong prognostic value. Patients with normal myocardial perfusion at exercise have an excellent prognosis regarding overall mortality and cardiovascular events. In the presence of exercise-induced perfusion defects, prognosis is impaired. Likely because of its higher spatial resolution, PET provides a better discrimination of low-risk from high-risk disease than SPECT (20) (Fig. 4).

As opposed to SPECT, which provides only qualitative evaluation of myocardial perfusion, PET can be used for quantitative measurement of myocardial blood flow at rest and during stress (measured in milliliter/gram/minute). The so-called coronary flow reserve can be obtained my dividing myocardial blood flow during stress by blood flow at rest and may be prognostically advantageous (21). Especially in patients with diabetes, SPECT imaging may miss so-called balanced ischemia in the presence of 3-vessel disease, and it is assumed that the quantitative measurement of myocardial blood flow may have diagnostic advantages in this patient group. In fact, Fiechter et al. (22) documented in 73 patients that the use of coronary flow reserve increased the sensitivity of perfusion PET from 79% to 96%, with an unchanged specificity of 80%, resulting in an improvement of the accuracy from 79% to 92%. Murthy et al. (23) performed a large trial that included 1,172 patients with diabetes and 1,611 normoglycemic individuals to analyze the prognostic value of coronary flow reserve measured by PET. After rest and dipyridamole imaging with the perfusion-traced rubidium-82, patients were followed for a median period of 1.4 years. The annualized rate of cardiovascular death was 7.6% in 600 patients with diabetes and impaired flow reserve (here assumed as a value ≤1.6), but only 1.3% in 572 diabetic patients with normal flow reserve (>1.6). In 339 patients with diabetes but no preexisting coronary disease and a normal coronary flow reserve, the cardiac mortality rate was only 0.3%. This was not significantly different from 759 individuals without diabetes and a normal coronary flow reserve (0.5%) (Fig. 5).

In a similar investigation, the same group of authors analyzed the value of myocardial flow reserve in 866 patients with moderate to severe impairment of renal function, which is known to be associated with an increased risk of coronary events. Patients were followed for a mean period of 1.28 years. After adjustment for all risk factors, cardiac mortality was more likely by a factor of 2.1 if flow reserve remained below the median (here: 1.5) (24).

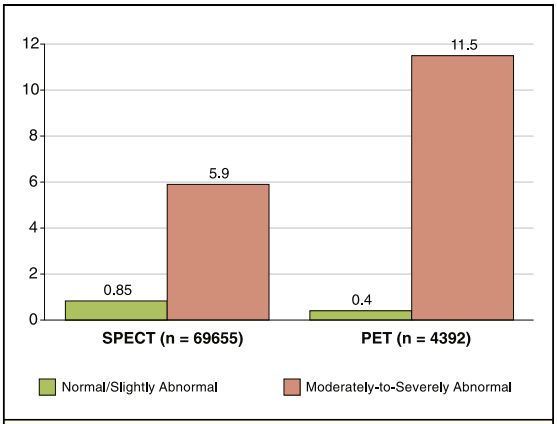

Figure 4. Prognostic Value of SPECT and PET

Results of a meta-analysis demonstrate the prognostic implications of a normal or slightly abnormal (low risk) versus moderately or severely abnormal (high risk) myocardial perfusion study of single-photon emission computed tomography (SPECT) and positron emission tomography (PET). A higher discriminatory power of PET is demonstrated. Modified from Shaw et al. (20).

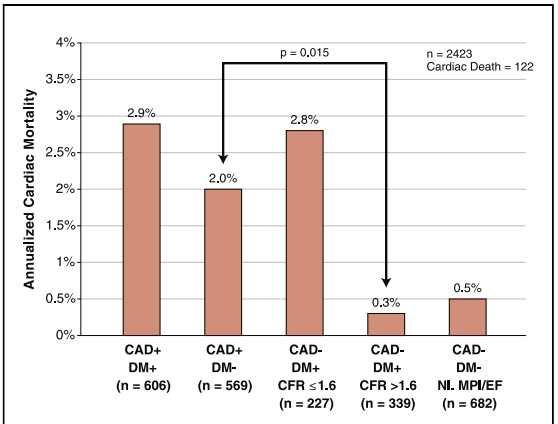

Figure 5. Impact of CFR Measured by Positron Emission Tomography on the Prognosis in Diabetic Individuals

The graph demonstrates the cardiac mortality rate in 2,423 individuals with and without diabetes, with and without pre-existing coronary artery disease (CAD), and with normal versus impaired myocardial flow reserve. It is demonstrated that diabetic individuals without pre-existing CAD are not a homogeneous population. Although the subgroup with impaired coronary flow reserve (CFR) has a cardiac mortality rate similar to that of those individuals with pre-existing CAD, diabetic patients with normal CFR have a prognosis similar to that of nondiabetic individuals. DM = diabetes mellitus; NI. MPI/EF = normal myocardial perfusion imaging and ejection fraction. Modified from Murthy et al. (23).

Myocardial perfusion imaging with PET and SPECT has strong prognostic power. PET has superior spatial resolution compared with SPECT and in addition permits the quantitative (as opposed to qualitative) measurement of myocardial perfusion. Coronary flow reserve, which can be obtained by dividing myocardial perfusion during exercise by perfusion at rest, has been shown to have strong prognostic power for cardiac mortality. Normal coronary flow reserve, even in high-risk patient groups such as those with diabetes, is associated with lower mortality.

A specific and important feature of nuclear cardiology methods is the fact that they can be used for molecular imaging. This means that by using specific tracers, molecular mechanisms, or structures such as cell surface receptors can be visualized. As an example, Bucerius et al. (25) could demonstrate that vascular nicotinic acetylcholine receptors can be visualized with specific antibodies that were marked by ^{18}F sodium fluoride (^{18}F) and that patients with Parkinson disease, even in the vascular system, have a lower concentration of receptors than healthy controls. Several other papers published in 2012 also highlighted the fact that cardiac PET provides insight into physiological and pathophysiological processes on a molecular level. As an example, it is assumed that ^{18}F is a marker for bone formation and active calcification, and it was demonstrated that increasing amounts of coronary artery calcification are associated with increasing coronary artery uptake of ^{18}F sodium fluoride (but not ^{18}F-fluorodeoxyglucose, a marker of metabolic activity in cardiac PET) (26). Similarly, in patients with aortic valve stenosis, increased ^{18}F activity was observed, with a closer association between ^{18}F activity (marker of calcification) and stenosis severity than between ^{18}F-fluorodeoxyglucose uptake (marker of inflammation) and stenosis severity (27).

Molecular imaging of the renin-angiotensin system could be of particular importance because it plays an important role in normal and pathological remodeling of the left ventricular myocardium after myocardial infarction. Interindividual variations of the renin-angiotensin system could explain why some patients display pronounced remodeling of the left ventricle (with ventricular dilation and reduced ejection fraction) and some others do not. It might also explain the variability of response to treatment with antagonists of the renin-angiotensin system. Dilsizian et al. (28) used lisinopril-labeled with technetium-99m to successfully image human myocardial tissue angiotensin-converting enzyme overexpression in transgenic rats by external micro SPECT/CT (28). Fukushima et al. (29) used a ^{11}C-labeled ligand to the AT1 receptor to study the regional expression of the AT1 receptor in pigs after myocardial infarction and in human control subjects by PET/CT. They found a regionally homogeneous uptake in healthy myocardium. In infarcted myocardium, the density was reduced.

However, after correcting for reduced flow in the infarcted areas, the specific receptor-associated activity was higher in infarcted areas compared with normal myocardium, indicating upregulation of the AT1 receptor in infarcted myocardium (Fig. 6). Similarly, expression of the receptor was increased in the remote myocardium of infarcted pigs compared with healthy controls. In healthy human individuals, olmesartan suppressed ligand uptake.

In the future, imaging of the renin-angiotensin system could not only provide in vivo scientific insight into the mechanisms of post-infarct remodeling, but, given the presence of interindividual variations, also help to identify targeted approaches to heart failure therapy in different individuals (30).

Because nuclear cardiology methods use radiotracers that actively emit signals (as opposed to, for example, the passive attenuation in CT), very low tracer concentrations can be detected. Suitable, selective, and specific tracers provide for visualization of molecular structures and processes and for the analysis of their regional distribution by SPECT and PET. Next to expanding scientific knowledge, such imaging approaches may help to select and guide targeted therapies in the future.

Cardiac Magnetic Resonance

CMR offers several major areas of application: imaging of cardiac morphology and function; analysis of myocardial perfusion during rest and stress; myocardial tissue characterization including imaging scar, infiltration, fibrosis, and iron; and magnetic resonance coronary angiography, which, however, remains technically challenging and is infrequently used in clinical practice.

Morphology and function. CMR is assumed to be the gold standard for noninvasive evaluation of cardiac morphology and function. It can be used to sensitively detect subtle changes in myocardial mass and global or regional contractile function. Recently, CMR was applied to analyze changes in global and regional left ventricular function in 20 patients with ischemic cardiomyopathy and therapy with cardiac stem cells harvested from the right atrial appendage during bypass surgery (31). In treated patients, there was significant improvement of left ventricular ejection fraction (from 27.5% to 35% after 4 months and 41% after 12 months) and especially pronounced improvement of myocardial segments with the greatest contractility at baseline. However, the results of the reported trial are incomplete

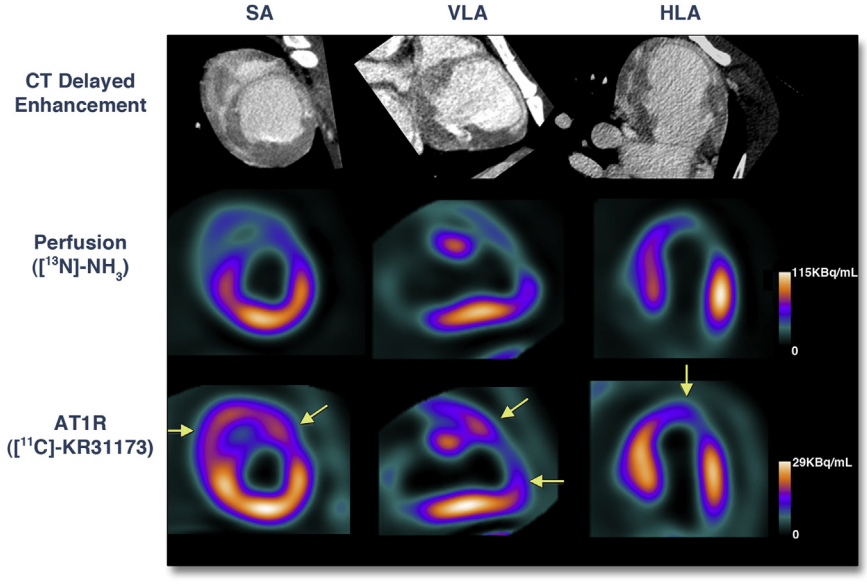

Figure 6. Visualization of Myocardial Perfusion and of the Regional Expression of the AT1R in a Pig After Anterior Myocardial Infarction

There is reduced activity of the tracer in infarcted myocardium. However, after correction for myocardial perfusion, tracer activity (and therefore receptor expression) is higher in infarcted myocardium compared with remote myocardium. AT1R = AT1 receptor; CT = computed tomography; HLA = horizontal long axis; SA = short axis; VLA = vertical long axis. Panel on right reprinted, with permission, from Fukushima et al. (29).

because no data on randomized control groups are available.

Myocardial perfusion. One of the most frequent clinical applications of CMR is the investigation of myocardial perfusion after intravenous injection of gadolinium during adenosine stress in first pass. It has high spatial resolution and can provide quantitative values of myocardial perfusion during rest and stress, similar to PET (32). In a study involving 41 patients with suspected coronary artery disease, CMR at 1.5-T was compared with PET to quantitatively analyze myocardial perfusion at rest and during adenosine stress (33). Both methods had similar discriminatory power to identify patients with high-grade coronary artery stenosis (PET: 92% sensitivity, 69% specificity, area under the curve = 0.81; CMR: 86% sensitivity, 76% specificity, AUC = 0.81). There was a good correlation of coronary flow reserve (absolute values of myocardial perfusion at stress divided by rest) measured with the 2 methods (r = 0.75). However, the absolute perfusion values at rest (r = 0.32) and during stress (r = 0.37) showed poor correlation, indicating the presence of unidentified, systematic differences between the 2 methods (Fig. 7).

In an investigation of 53 patients, Jogya et al. (34) validated adenosine stress CMR with a 3-T system against invasively measured fractional flow reserve (FFR), the invasive gold standard for identifying hemodynamically relevant coronary artery stenoses. CMR demonstrated a sensitivity of 91% and a specificity of 90% for the identification of patients who had at least 1 stenosis with an invasive FFR ≤0.75. For the identification of specific coronary arteries with a relevant stenosis (FFR ≤0.75), sensitivity was 79% and specificity was 92%. In a similar study

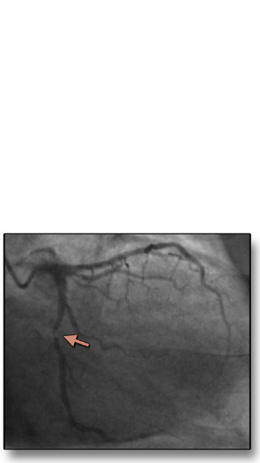

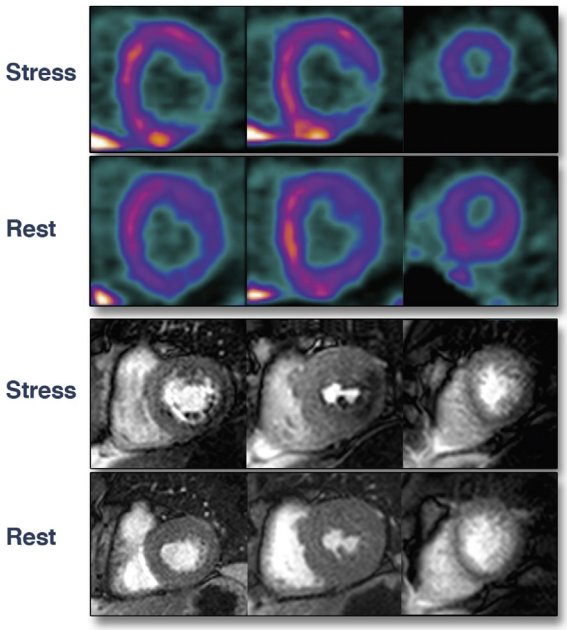

MPR2	LAD	CX	RCA
PET	1.7	1.3	1.97
CMR	1.9	1.42	1.87

Figure 7. Assessment of Myocardial Perfusion at Rest and During Adenosine Stress With ^{13}N Ammonia PET and 1.5-T CMR in 41 Patients With Suspected Coronary Artery Disease

(Top) Perfusion defect in the posterolateral wall in a patient with high-grade stenosis of the left circumflex artery (LX). **(Bottom)** Poor correlation of absolute perfusion values during stress by cardiac magnetic resonance (CMR) and positron emission tomography (PET) (**left**, r = 0.37), good correlation of coronary flow reserve (r = 0.75) and similar discriminatory power of CMR and PET regarding the identification of patients with stenoses ≥70%. MPR2 = myocardial perfusion reserve for the lowest 2 segments of each territory; LAD = left anterior descending artery; RCA= right coronary artery. Panel on right reprinted, with permission, from Morton et al. (33).

that included 120 patients studied with a 1.5-T system, 90% sensitivity and 82% specificity were found (35).

The CE-MARC (Clinical Evaluation of Magnetic Resonance Imaging in Coronary Heart Disease) study, performed in Leeds, United Kingdom, received widespread attention. In 752 patients with suspected coronary artery disease, a combined CMR protocol including rest and stress myocardial perfusion, left ventricular function, late gadolinium enhancement (LGE) imaging to identify scar, and magnetic resonance coronary angiography was compared with rest/stress SPECT myocardial perfusion imaging regarding the identification of coronary artery stenoses (36). The combined CMR protocol had 86.5% sensitivity and 83.4% specificity. For SPECT, 66.5% sensitivity and 82.6% specificity were reported. MR coronary angiography, however, was assessable in only 55% of patients. If the results of magnetic resonance coronary angiography were not taken into account, sensitivity of magnetic resonance was 81.6% and specificity was 85.9% (with, however, wide confidence intervals [CIs] so that it cannot be concluded that magnetic resonance coronary angiography significantly improved the results of the combined magnetic resonance protocol). The authors concluded that CMR is superior to SPECT for the identification of patients with significant coronary artery disease. The study is not undisputed, and some concerns have been raised concerning SPECT technique and interpretation (37) and the lack of a core laboratory evaluation despite a single-center design.

Jaarsma et al. (38) performed a systematic meta-analysis comparing the diagnostic performance of myocardial perfusion imaging with SPECT, PET, and CMR to identify patients with relevant coronary artery stenoses based on 166 published articles. The 3 methods had a similarly high specificity (84% to 89%), but specificity varied (61% for SPECT, 76% for CMR, and 81% for PET) (Table 1, Fig. 8).

Table 1. Diagnostic Value of SPECT, CMR, and PET to Identify Patients With Coronary Artery Stenosis

	No. of Publications	Sensitivity, % (95% CI)	Specificity, % (95% CI)	DOR (95% CI)
SPECT	105	88 (88–89)	61 (59–62)	15.3 (12.7–18.5)
CMR	7	89 (88–91)	76 (73–78)	26.4 (17.7–39.5)
PET	11	84 (81–87)	81 (74–875)	36.5 (21.5–61.9)

Reprinted, with permission, from Jaarsma et al. (38).
CI = confidence interval; CMR = cardiac magnetic resonance; DOR = diagnostic odds ratio; PET = positron emission tomography; SPECT = single-photon emission computed tomography.

The authors concluded that SPECT is inferior regarding specificity, the diagnostic performance of CMR and PET are similar, and the criteria for selecting the appropriate test for a given patient should include radiation exposure and local expertise.

CMR myocardial perfusion is a valuable method to identify hemodynamically relevant coronary artery stenoses. Performed and interpreted with expertise, it has a diagnostic performance similar to that of PET and allows accurate quantification of myocardial perfusion reserve (Fig. 8). Compared with invasive coronary angiography, however, an excellent agreement cannot be expected for any myocardial perfusion imaging modality (whether with SPECT, PET, or CMR) because coronary angiography is not a functional test and thus cannot detect or demonstrate ischemia. Not every coronary artery stenosis associated with a high-grade diameter reduction actually causes myocardial perfusion deficits or ischemia.

Myocardial tissue characterization. CMR tissue characterization includes LGE imaging, which constitutes an integral part of most CMR studies. It reliably visualizes myocardial scar, fibrosis, infiltration such as in cardiac amyloidosis, and other chronic myocardial alterations. Importantly, LGE carries significant prognostic relevance. In a population cohort from Iceland, 936 elderly inhabitants (67 to 93 years of age) were subjected to magnetic resonance LGE imaging (39). In addition to 91 clinically known myocardial infarctions, CMR identified scars subsequent to clinically unnoticed myocardial infarction in a further 157 patients. During 6 years of follow-up, the mortality rate was 33% in patients with clinically known myocardial infarction, 28% in patients with previously unrecognized scars as detected by CMR, and 17% in patients with normal findings on LGE imaging. Abnormalities in LGE imaging remained significantly associated with mortality after adjustment for age and risk factors.

An important area of application for LGE imaging is the assessment of viability in areas of myocardial ischemia and infarction, specifically the question whether a specific region will regain or improve contractile function after revascularization. The extent of transmurality of late enhancement as seen in magnetic resonance imaging is related to the probability of functional recovery after coronary revascularization (40). However, not only LGE imaging, but also dobutamine stress CMR can be used to assess viability, in which return of contractile function under low-dose dobutamine infusion predicts improvement after revascularization. In a

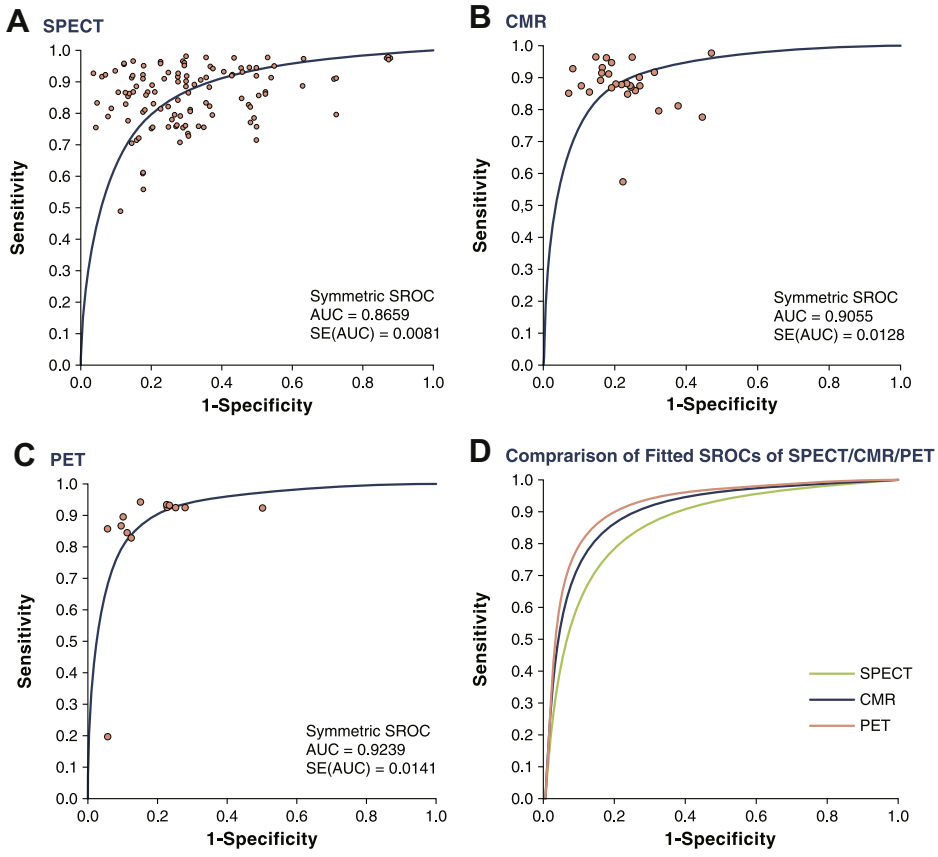

Figure 8. Diagnostic Accuracy of Imaging Modalities for Myocardial Perfusion Regarding the Detection of Coronary Artery Disease

The graphs indicate the accuracy for coronary artery disease detection in the form of receiver-operating characteristics curves for SPECT **(A)**, CMR **(B)**, PET **(C)**, and a comparison of all 3 curves within 1 graph **(D)**. AUC = area under the curve; SROC = symmetric receiver-operating characteristics curve; other abbreviations as in Figures 4 and 7. Reprinted, with permission, from Jaarsma et al. (38).

meta-analysis of 24 studies with 698 patients, Romero et al. (41) compared LGE and dobutamine stress CMR to identify viable infarct areas. Although LGE CMR displayed higher sensitivity (95% vs. 81%), dobutamine stress CMR had a higher specificity (91% vs. 51%).

The prognostic relevance of revascularization of viable and nonviable myocardium was investigated in a trial encompassing 144 patients with a left ventricular ejection fraction ≤35% (42). The authors demonstrated that purely medical therapy in patients with viable myocardium was associated with a worse prognosis than in patients without viable myocardium (3-year survival rate: 48% vs. 77%, $p = 0.02$). If revascularization was performed, prognosis was not influenced by the absence or presence of viable myocardium. A subanalysis of 43 matched patient pairs showed that in the presence of viable myocardium, the 3-year mortality risk was significantly higher for patients without revascularization compared with patients in whom revascularization was performed (HR: 2.5, 95% CI: 1.1 to 6.5) (Fig. 9).

The combination of severe systolic dysfunction and viable myocardium as assessed by CMR seems to be a risk factor for mortality if patients are not revascularized.

Abnormal findings in LGE imaging are not limited to myocardial infarction. Fibrosis in the context of other diseases can also cause such abnormalities: in combination with other findings, including myocardial edema, LGE in CMR is an important method to identify acute myocarditis (although less useful for chronic myocarditis [43]). LGE is also found, for example, in dilated cardiomyopathy, hypertrophic cardiomyopathies, sarcoidosis, and amyloidosis. Confirming several previous studies, Levya et al. (44) demonstrated prognostic relevance in nonischemic cardiomyopathies. In 97

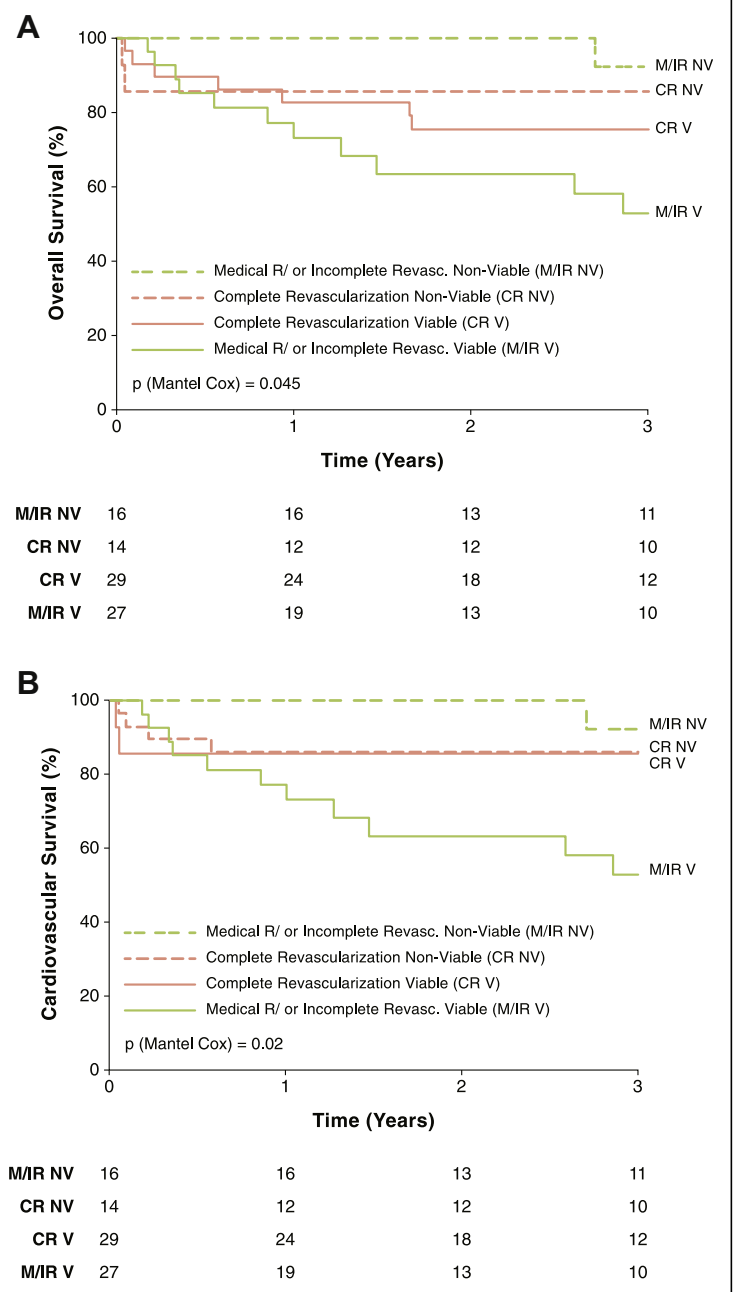

Figure 9. Late Enhancement and Prognosis in Patients With Reduced Ejection Fraction

Viability assessed by CMR LGE imaging, revascularization and 3-year mortality in 43 matched patient pairs, all with a left ventricular ejection fraction ≤35%. In the presence of viable myocardium (CR V and M/IR V), 3-year survival is significantly reduced if no revascularization is performed (M/IR V). Reprinted, with permission, from Gerber et al. (42).

patients who underwent resynchronization therapy, the HR for cardiac mortality was 18.6 (95% CI: 3.5 to 98.5) if fibrosis was detectable by LGE imaging (44) (Fig. 10).

Observations in a group of 137 patients scheduled for placement of an automated implantable cardioverter-defibrillator (ICD) point in the same direction. The presence (and extent) of abnormalities in CMR LGE images was a predictor for the endpoint death or adequate ICD discharge, both in patients with ischemic cardiomyopathy and in patients with nonischemic cardiomyopathy (45) (Fig. 11).

In patients with hypertrophic cardiomyopathy, high signal intensity areas on LGE images indicate fibrosis and can be observed frequently. Their extent is progressive over time (46). Based on a meta-analysis of 4 previously published trials, Green et al. (47) report that these areas were present in 60% of 1,063 patients with hypertrophic cardiomyopathy (the pattern is typically of patchy nature and more pronounced in areas of myocardial hypertrophy). For several endpoints, including cardiovascular mortality and total mortality (odds ratio [OR]: 4.46), the presence of LGE was significantly predictive. For the prediction of the combined endpoint sudden cardiac death or adequate ICD discharge, the OR was 2.35 and, with a 95% CI from 0.87 to 6.58, just missed significance ($p = 0.091$). This is of clinical relevance because the prediction of sudden death in patients with hypertrophic cardiomyopathy is difficult and markers of increased risk that help to identify patients who would benefit from ICD therapy or in whom it could safely be avoided would be very useful. Interestingly, LGE can even be found in genotype-positive, but phenotype-negative relatives of hypertrophic cardiomyopathy patients (48). Clinical implications of this observation are still unclear.

A strong predictive value of LGE imaging was also shown in patients with myocarditis. In a study of 222 patients who were followed on average for 4.7 years, Grün et al. (49) demonstrated high all-cause (19.2%) and cardiac (15%) mortality rates in the presence of LGE abnormalities. The presence of LGE had an HR ratio of 8.4 for all-cause mortality and 12.8 for cardiac mortality, independent of clinical symptoms. Importantly, this is superior to left ventricular ejection fraction, end-diastolic volume, or New York Heart Association functional class with HRs between 1.0 and 3.2 for all-cause and between 1.0 and 2.2 for cardiac mortality rates (49).

In patients with nonischemic myocardial disease, the presence of LGE indicates irreversible injury, which is clinically important. Numerous studies in patients with various clinical conditions demonstrate the prognostic relevance of the presence and extent of LGE. In the future, LGE could be a key parameter for determining the need for ICD placement.

Recently, the direct measurement of magnetic relaxation times has received a lot of attention.

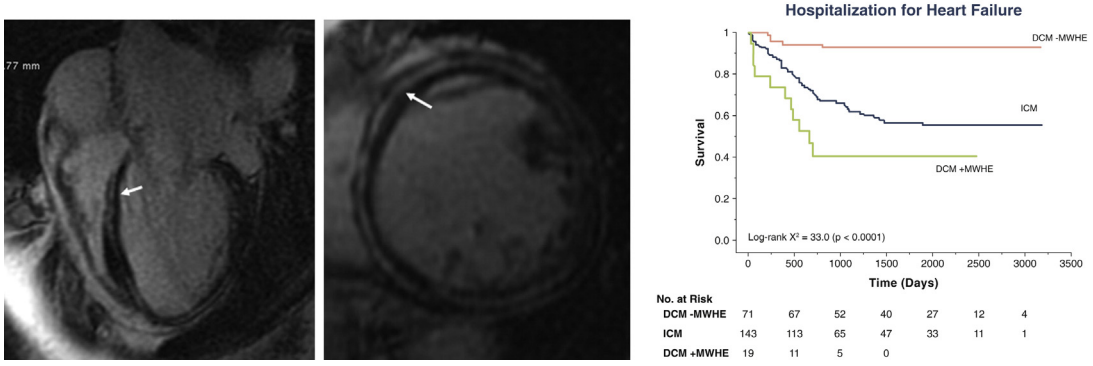

Figure 10. Typical Mid Wall Sign Obtained by Late Gadolinium Enhancement in a Patient With Nonischemic Cardiomyopathy

In 97 patients with nonischemic cardiomyopathy **(left, arrows)** scheduled for resynchronization therapy, the presence of abnormal hyperenhancement (DCM + MWHE) was associated with a significantly worse prognosis compared with patients without detectable hyperenhancement (DCM − MWLE). The cardiovascular survival curve of patients with ischemic cardiomyopathy (ICM) was between the former 2 groups. DCM = dilated cardiomyopathy; MWHE = midwall hyperenhancement. Reprinted, with permission, from Levya et al. (44).

Because the relaxation properties of myocardial tissue is the underlying mechanism for pathology-specific signal intensity changes in images, the mapping of these times (mainly T1, T2, and T2*) may overcome problems of signal intensity–based imaging and allow absolute normal and cutoff values to be established for a more accurate detection of tissue abnormalities. Mapping techniques have been shown to provide accurate information on the extent of abnormalities in ischemic and nonischemic heart disease (50–54), but although they have been validated and have the potential to replace many of the current signal intensity–based magnetic resonance imaging approaches (55), the acquisition techniques and evaluation procedures are not yet standardized.

Magnetic resonance coronary angiography. Because of its relatively limited spatial and contrast resolution, imaging of the coronary arteries by magnetic resonance angiography remains challenging and is not incorporated into clinical routine, except for the characterization of coronary anomalies or the identification of large coronary aneurysms as a consequence of Kawasaki disease. In the CE-MARC trial described previously, addition of the results of CMR coronary angiography to the other CMR findings had some effect on sensitivity and specificity, but did not significantly improve accuracy. Furthermore, it was assessable in only 55% of patients (36). Image quality is substantially lower than for CT coronary angiography (Fig. 12). However, most coronary artery events are caused by atherosclerotic lesions in the proximal segments of the coronary system and, with adequate hardware and technique, the proximal coronary segments can be visualized relatively reliably by CMR. Correspondingly, Yoon et al (56), who studied 207 patients by magnetic resonance whole-heart free-breathing coronary angiography on a 1.5-T system and followed the cohort for 25 months, observed 5 severe cardiac events (1 cardiac death and 4 cases of unstable angina) in 84 patients with significant stenosis in the proximal coronary artery segments, whereas of 123 individuals without proximal stenosis, none had a severe event (56).

Although magnetic resonance coronary angiography continues to be a subject of ongoing research, image quality is often significantly impaired in clinical routine, and the method plays no routine role for the identification of coronary stenoses.

Real-time CMR. With suitable systems, magnetic resonance imaging can be performed in real time and can be used for catheter guidance in a manner similar to fluoroscopy. Ratankaya et al. (57) have been able to show that right heart catheterization can be performed under magnetic resonance guidance and that gadolinium-filled balloons at the catheter tip provide better imaging than balloons filled with air. Similarly, the use of magnetic resonance has been reported for the real-time guidance of catheter placement (58,59), but the method is not considered ready for clinical application.

The use of real-time CMR is a potential concept for radiation-free, 3D catheter guidance to support cardiac interventions in the future.

Cardiac CT

The minimum prerequisite for cardiac CT is a CT system with at least 64 detector rows, fast rotation,

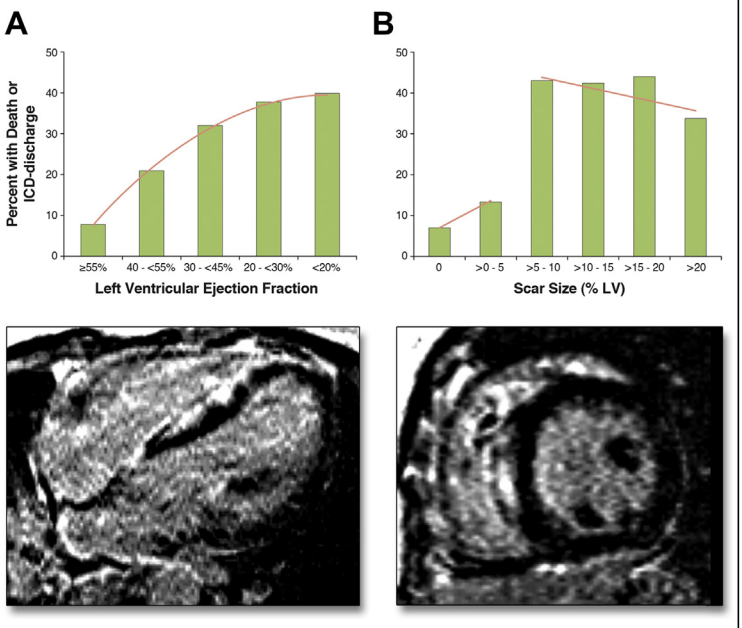

Figure 11. Patient With Nonischemic Pattern of Late Gadolinium Enhancement on Magnetic Resonance Imaging

Event rate (death or adequate implantable cardioverter-defibrillator [ICD] discharge) depending on left ventricular systolic function **(A)** and extent of late enhancement **(B)**. Modified, with permission, from Klem et al. (45).

and the ability to perform electrocardiography-synchronized data acquisition or reconstruction. Technology is progressing continuously. On the one hand, systems with as many as 320 detector rows have become available, which in many cases permit coverage of the entire volume of the heart in a single cardiac cycle. On the other hand, systems that combine 2 x-ray tubes and detector arrays (dual-source CT) have been developed and improve temporal resolution by a factor of 2 compared with systems with a single x-ray tube. The major targets of cardiac CT imaging are the coronary arteries because other noninvasive imaging methods do not permit imaging of the coronary vessels with comparable image quality.

Coronary calcium. For many years, CT has been used to detect and quantify coronary artery calcium. Coronary calcium is a marker of coronary atherosclerotic plaque and is associated with an increased risk of future cardiovascular events, as demonstrated by earlier landmark studies (51) and confirmed, in various subgroups, by recent trials and analyses (60–63). Yeboah et al. (64) compared the predictive value of various novel risk markers in a population-based study with 6,814 participants. Over a mean follow-up period of 7.6 years, 94 cardiac events occurred (myocardial infarction, angina with revascularization, and coronary death). In a multivariable analysis, only coronary calcium detected by CT (HR: 2.60, 95% CI: 1.94 to 3.50, $p < 0.001$) and a family history of premature heart disease (HR: 2.18, 95% CI: 1.38 to 3.42, $p < 0.001$) were associated with future events, whereas the ankle-brachial index (HR: 0.79), brachial vasoreactivity (HR: 0.93), carotid intima–media thickness (HR: 1.17), and highly sensitive C-reactive protein (HR: 1.28) were not independently predictive.

Coronary CT angiography. In the past decade, coronary CT angiography has become a much more prominent application of cardiac CT than coronary calcium scoring. The main clinical benefit is derived from the high negative predictive value of coronary CT angiography. The ability to reliably rule out stenosis makes CT a useful tool to rule out significant coronary artery disease in symptomatic patients with a low pre-test likelihood of disease. This potentially includes many individuals with acute chest pain who are often at low risk of actually having an acute coronary syndrome, whereas, on the other hand, a missed diagnosis may have severe consequences. In 2012, 2 large trials investigated the clinical value of coronary CT angiography in this situation. Litt et al. (65) randomized 908 of 1,370 patients with acute chest pain to undergo coronary CT angiography. Of these 908 patients, 640 could be immediately discharged after negative findings on a CT scan and within the following 30 days, no deaths or myocardial infarctions occurred. However, the overall rate of events was low: only 10 of 908 patients in the CT group (all with positive findings on CT) and 5 of 464 patients in the traditional care group experienced a myocardial infraction within the 30-day follow-up period (1% in each group). Hoffmann et al. (66) randomized 1,000 low-risk acute chest pain patients in a multicenter trial, so that 501 patients underwent coronary CT angiography as an initial test; 50% of these patients were discharged from the emergency department within 8.6 h (as opposed to 26.7 h in the traditional care group). No patient with negative findings on CT (no stenosis >50%) experienced acute myocardial infarction. Similar to the previous study, the patients mainly had a low risk, and only 23 myocardial infarctions occurred in the entire patient cohort (plus 52 cases of unstable angina).

In patients with stable chest pain, coronary CT angiography is also prognostically relevant. Numerous publications from the CONFIRM registry, with a total enrolled patient number of more

than 32 000, have demonstrated low total mortality and cardiac event rate if coronary CT angiography showed no coronary stenosis and no coronary atherosclerotic plaque (67). The severity of coronary artery disease as documented by coronary CT angiography has prognostic implications. It could be shown that symptomatic patients with "high-risk anatomy" (left main stenosis, 3-vessel disease or 2-vessel disease with involvement of the proximal LAD) profit from revascularization, while patients with lower-risk coronary anatomy do not (68). In a similar trial including 2,977 patients, Cho et al. (69) demonstrated that in patients with suspected coronary artery disease, coronary CT angiography (maximum degree of stenosis) had a higher prognostic value than stress electrocardiography (69).

An important question is whether coronary CT angiography could (and should) also be used for risk stratification of asymptomatic individuals. Within the CONFIRM registry, 7,590 patients without chest pain could be identified. Coronary CT angiography was prognostically relevant in these individuals. After adjustment for Framingham risk score, patients with stenoses >50% in 2 or 3 vessels (but not patients with a stenosis only in 1 vessel or lesions that were not considered hemodynamically relevant) had a worse prognosis (70). However, HRs were relatively low (2.2 for 2-vessel disease and 2.9 for 3-vessel disease). Of particular interest is the observation that after adding coronary calcium to the Framingham risk score, coronary CT angiography did not incrementally improve risk stratification (70).

Coronary CT angiography has a high accuracy for detection of coronary artery stenoses. There is a growing body of evidence concerning prognostic implications of coronary CT angiography. Uniformly, the trials report very good prognosis when coronary CT angiography findings are normal. However, most of the respective studies and analyses were performed in patient groups with a very low baseline risk, so that even with abnormal findings on CT, the risk is increased, but not greatly. Studies in patient groups with higher baseline risk will be necessary to better understand the overall prognostic potential of coronary CT angiography.

Late enhancement, CT perfusion, and FFR. In a fashion similar to CMR, contrast-enhanced CT permits investigation of myocardial contrast enhancement. Instead of gadolinium, iodinated contrast agent is used, which displays kinetics similar to those of gadolinium. Myocardial perfusion can be analyzed in first pass, and areas of scar and fibrosis cause late enhancement. In case of acute coronary interventions, the contrast injected during the invasive coronary procedure can be used to assess late enhancement by CT. Sato et al. (71) demonstrated in 102 patients with a first myocardial infarction that the extent of late enhancement quantified immediately after the acute intervention correlates with the prognosis during the next 24 months (Fig. 13).

Regarding first-pass assessment of myocardial perfusion, some earlier work in small patient groups is available from previous years. In 2012, George et al. (72) investigated 50 patients in a 320-slice system. The authors aimed to clarify whether adding CT myocardial perfusion to CT coronary angiography would improve agreement with SPECT myocardial perfusion imaging. As expected, the agreement of SPECT and CT angiography alone was not very good; CT angiography had a sensitivity of 56% and specificity of 75% for the identification of SPECT perfusion defects. CT perfusion imaging had closer agreement: 72% sensitivity and 91% specificity. The most valid comparison standard is invasive coronary angiography with FFR measurement. Ko et al. (73) validated coronary CT angiography with and without additional CT myocardial perfusion during adenosine stress in 40 patients compared with invasive coronary angiography and FFR (73). For the detection of coronary stenosis that was hemodynamically relevant (FFR ≤0.8), sensitivity of coronary CT angiography alone was 95% and specificity was 78%. By adding CT perfusion,

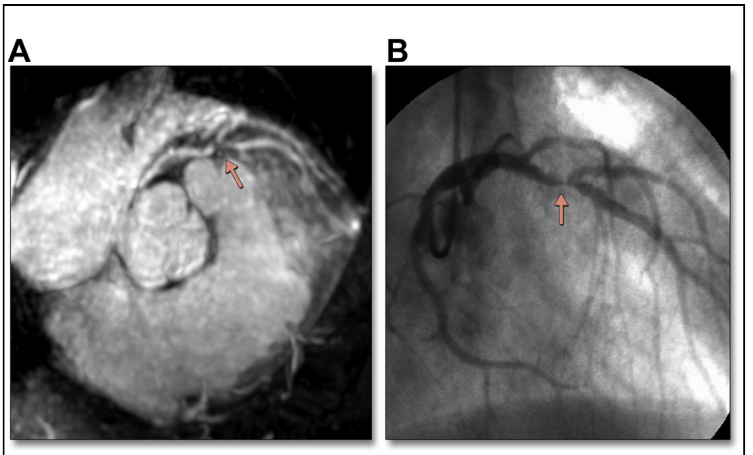

Figure 12. Magnetic Resonance Coronary Angiography With a 1.5-T System Acquired Without Intravenous Contrast in Free Breathing

(A) Magnetic resonance. **(B)** Corresponding invasive coronary angiogram. The **arrows** indicate stenosis of left anterior descending coronary artery. Reprinted, with permission, from Yoon et al. (56).

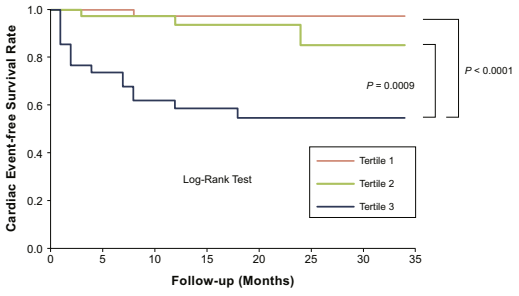

Figure 13. Late Enhancement in a Patient After Acute Anterior Myocardial Infarction, Here Color-Coded in Red

The image was acquired immediately after acute PCI, without additional contrast injection. Total mass of infarcted area is 63.4 g. Curves of survival free of further cardiac events (cardiac death and heart failure) depending on the overall mass of infarcted territory as quantified by computed tomography late enhancement. Tertile 1: <11 g; Tertile 2: 11 to ≤36 g, Tertile 3: ≥36 g. Reprinted, with permission, from Sato et al. (71).

sensitivity was reduced to 87%, but specificity increased to 95% (Fig. 14).

In addition to the analysis of perfusion through direct visualization of myocardial enhancement during adenosine stress imaging, computationally elaborate simulations permit to obtain FFR values from anatomic coronary CT angiography data acquired at rest (74,75) (Fig. 15). After the initial results of this method had been presented in the relatively small DISCOVER-FLOW (Diagnosis of Ischemia-Causing Stenoses Obtained Via Noninvasive Fractional Flow Reserve) trial in 2011 (76), the results of a larger follow-up trial (DeFACTO [Determination of Fractional Flow Reserve by Anatomic Computed Tomographic Angiography] trial) were presented in 2012. In 252 patients, CT angiography with determination of FFR_{CT} was compared with catheter-based coronary angiography with invasive measurement of FFR (77).

In this trial, the sensitivity of FFR_{CT} to identify patients with at least 1 stenosis that had an invasively measured FFR value <0.8 was 90%, but specificity was only 54%. For coronary CT angiography alone, without consideration of FFR_{CT}, sensitivity was 84% and specificity was 42%. Overall, the results of the DeFACTO trial were a little worse than the results of the initial, smaller DISCOVER-FLOW study. More data from various centers, however, will be

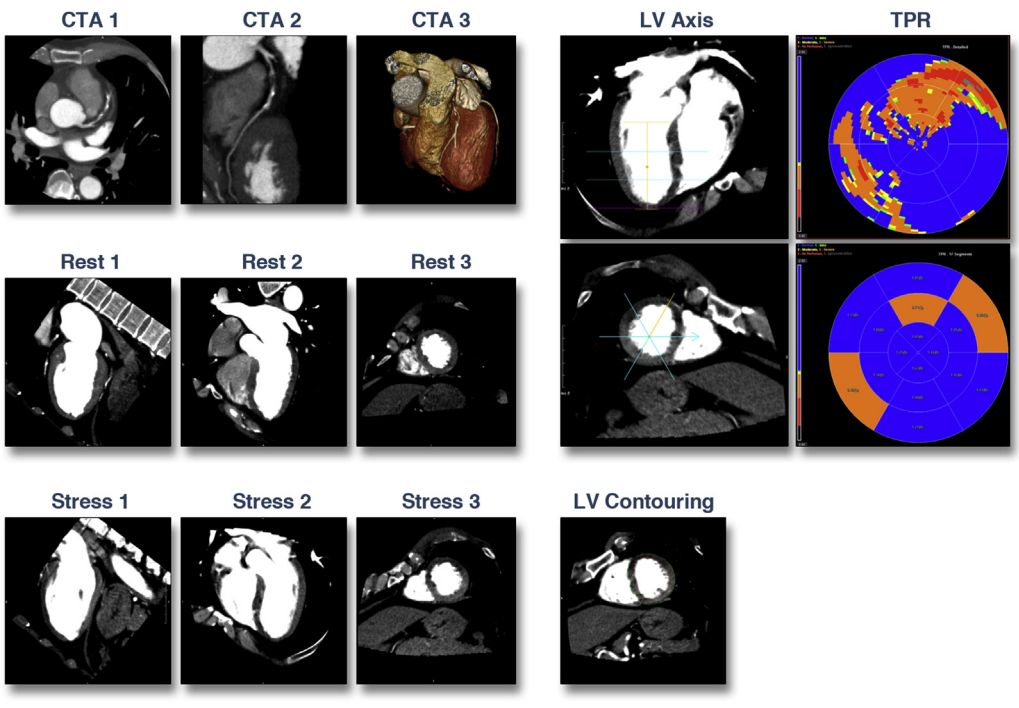

Figure 14. Adenosine Stress CT Myocardial Perfusion Imaging

The images demonstrate myocardial hypoperfusion in the left anterior descending artery territory **(arrow)** in contrast-enhanced computed tomography (CT) perfusion imaging under adenosine stress. Reconstructions are created in typical orientations, and the hypoenhanced myocardium can clearly be distinguished from normally perfused myocardium, which has higher CT attenuation. Reprinted, with permission, from Ko et al. (73).

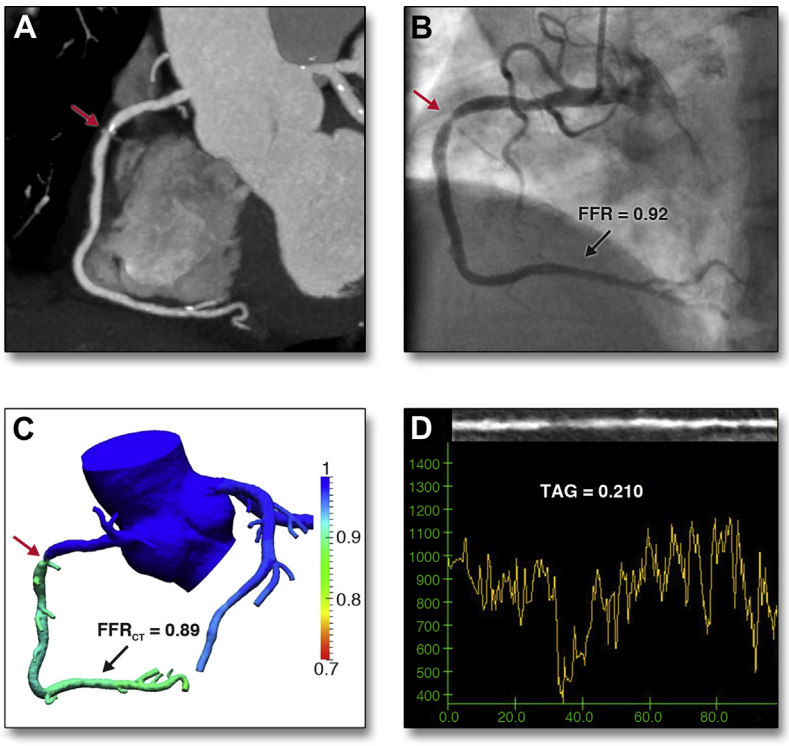

Figure 15. Fractional Flow Reserve Determination by Coronary CT Angiography

CT angiography **(A)**, invasive coronary angiography **(B)**, and CT-derived fractional flow reserve **(C)** in a patient with a proximal right coronary artery stenosis **(arrows)**. Both invasive fractional flow reserve (FFR) (0.92) and CT-derived fractional flow reserve (FFR_{CT}) (0.89) indicate that the stenosis is not hemodynamically relevant. The example is taken from a trial in which invasively measured FFR and FFR_{CT} were compared in 53 patients (74) and good agreement was found (area under the curve = 0.94). In this trial, FFR_{CT} was also compared with the transluminal attenuation gradient (TAG) **(D)**, a further measure that has been suggested to assess the hemodynamic relevance of coronary artery stenoses by CT (75), and FFR_{CT} proved superior (area under the curve for TAG: 0.63; $p < 0.001$), but the advantage of FFR_{CT} was no longer significant if analysis was limited to calcified vessels (area under the curve = 0.92 for FFR_{CT} vs. 0.75 for TAG and 0.80 for stenosis assessment by CT angiography alone). The Editors thank James Min of Weil-Cornell Medical College, New York, for providing the figure.

required to precisely define the clinical utility of CT-based FFR measurements.

Myocardial perfusion during adenosine stress imaging and FFR_{CT} serve to add functional information to the purely anatomic information obtained by coronary CT angiography. This may serve to reduce the false-positive rate of coronary CT angiography. This false-positive rate is partly caused by the limited spatial and temporal resolution of CT, making some lesions appear anatomically more high grade than they actually are, and partly caused by the fact that not all stenoses with a diameter reduction >50% or even >70% cause ischemia, and, by necessity, the correlation between anatomic and functional tests for coronary artery disease can never be perfect.

Atherosclerotic plaque. By CT, not only the coronary artery lumen but, image quality permitting, coronary atherosclerotic plaque can also be visualized and analyzed. Coronary plaque in CT angiography has been shown to have prognostic relevance (78–80). In the context of refined risk stratification, not only the presence of plaque, but more specifically the identification of vulnerable plaque—lesions that have a high likelihood to rupture or erode and cause acute coronary syndromes in the future—is of particular interest. Previous work has demonstrated that CT characteristics of such lesions include the absence of bulky calcification, the presence of positive remodeling, and low CT attenuation (<30 Hounsfield units) within the plaque (81). In addition, spotty calcification, even though not sharply defined, has repeatedly been mentioned as a marker of vulnerable plaque. In an ex vivo investigation of 21 coronary arteries, Maurovich-Horvat et al. (82) demonstrated that the napkin-ring sign, a ringlike

enhancement after contrast injection, was present in 38 of 238 plaques and that this sign had a very high specificity (98.9%) for the presence of advanced plaque in histology. Watabe et al. (83) investigated 107 patients in whom percutaneous coronary intervention was performed because of stable chest pain. Coronary CT angiography was performed in all patients before percutaneous coronary intervention. Although post-procedural troponin increase developed in 36 patients, it did not develop in 71. In patients with increased troponin, the target lesion had a significantly larger remodeling index on CT (1.20 vs. 1.04), it more frequently showed spotty calcification (50% vs. 11%), and the lesion had a significantly lower density (43 vs. 94 Hounsfield units) than in patients without a troponin increase. On multivariable analysis, spotty calcification (OR: 4.27) and positive remodeling (OR: 4.54) were independent predictors of troponin increase (Fig. 16).

If image quality is sufficient, CT permits the analysis of coronary atherosclerotic lesions regarding properties that are associated with plaque vulnerability. Whether these characteristic properties permit clinical risk stratification and identification of at-risk individuals requires further evaluation.

Catheter-based aortic valve replacement. Transcatheter aortic valve replacement has developed into a major application for cardiac CT. In this context, CT is used to obtain information about peripheral access, to identify obstacles in the aorta, and to obtain the exact dimensions of the aortic root (84). Several earlier publications demonstrated that CT provides different dimensions of the aortic root and especially of the aortic annulus than does echocardiography (85). Based on retrospective analyses, they suggested that CT-based sizing of the implanted prosthetic aorta might be superior to echocardiography-based sizing, with beneficial effects on the prevalence of post-procedural aortic regurgitation (which, in turn, is a relevant predictor of outcome [86]). In 2012, this was also demonstrated in a prospective trial (87). Jilaihawi et al. (87) used 2D transesophageal echocardiography (TEE) to measure the aortic annulus and choose the prosthesis size in 96 patients; they used CT in 40 different patients in whom prosthesis size was chosen according to the perimeter of the aortic annulus measured on CT. Paravalvular aortic regurgitation of more than a mild degree was present in 7.5% of patients with CT-based sizing and 21.9% of patients with TEE-based sizing. Similarly,

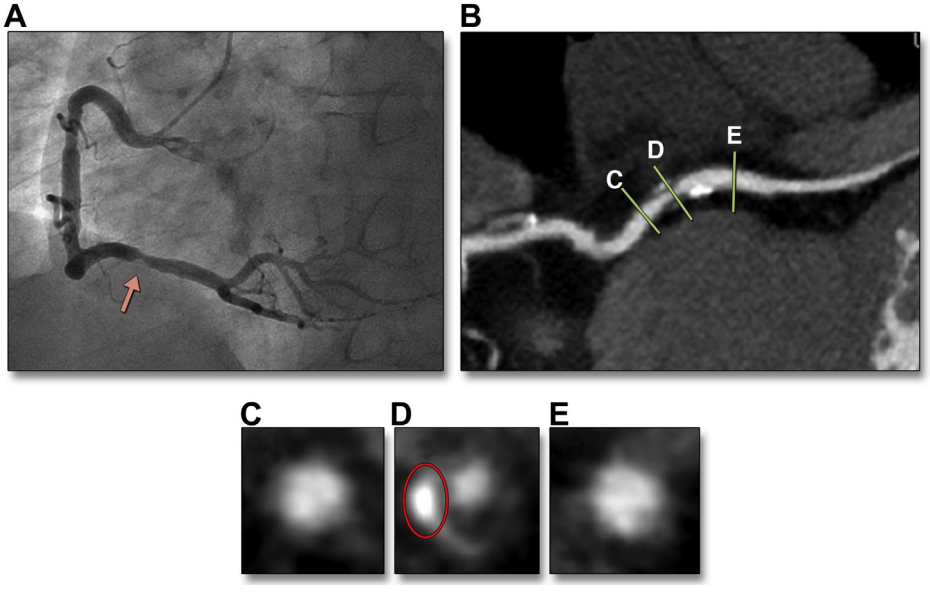

Figure 16. Invasive Coronary Angiography and Coronary CT Angiography of a Right Coronary Artery Lesion, the PCI of Which Led to Post-Procedural Troponin Increase

Invasive coronary angiography **(A)** and coronary CT angiography **(B)**. In CT, the typical features of "vulnerable plaque" are identifiable (**C, D,** and **E** which demonstrate serial cross-sections of the lesion in CT angiography). There is positive remodeling (remodeling index 1.28), "spotty calcification," and low CT attenuation (16 HU). The lesion also demonstrates the "napkin ring sign" **(D)**, even though this was not a specific area of investigation in this trial. Reprinted, with permission, from Watabe et al. (83).

Hayashida et al. (88) showed that CT-based sizing resulted in a prosthesis size on average 0.8 mm larger than TEE-based sizing and that it was associated with a lower rate of severe paravalvular regurgitation. A further piece of clinically useful information that can be obtained from CT is the prediction of suitable fluoroscopic projection angles that yield an orthogonal view of the aortic valve plane (89,90). This is of importance because it may lower the amount of contrast agent that is necessary to perform the implantation procedure.

CT is an important imaging modality in the workup of patients scheduled for transcatheter aortic valve replacement. A consensus document of the Society of Cardiovascular Computed Tomography summarizes relevant aspects and state of the art (84).

Reprint requests and correspondence: Dr. Stephan Achenbach, Department of Internal Medicine I (Cardiology), University of Giessen, Klinikstrasse 33, Giessen NA 35392, Germany. *E-mail: stephan.achenbach@uk-erlangen.de.*

REFERENCES

1. Gebhard C, Stahli BE, Greutmann M, Biaggi P, Jenni R, Tanner FC. Reduced left ventricular compacta thickness: a novel echocardiographic criterion for non-compaction cardiomyopathy. J Am Soc Echocardiogr 2012;25:1050–7.
2. Oxborough D, Sharma S, Shave R, et al. The right ventricle of the endurance athlete: the relationship between morphology and deformation. J Am Soc Echocardiogr 2012;25:263–71.
3. Zile MR, Gottdiener JS, Hetzel SJ, et al. Prevalence and significance of alterations in cardiac structure and function in patients with heart failure and a preserved ejection fraction. Circulation 2011;124:2491–501.
4. Russo C, Jin Z, Homma S, et al. Left atrial minimum volume and reservoir function as correlates of left ventricular diastolic function: impact of left ventricular systolic function. Heart 2012;98:813–20.
5. Welles CC, Ku IA, Kwan DM, Whooley MA, Schiller NB, Turakhia MP. Left atrial function predicts heart failure hospitalization in subjects with preserved ejection fraction and coronary heart disease: longitudinal data from the Heart and Soul Study. J Am Coll Cardiol 2012;59:673–80.
6. Lancellotti P, Magne J, Donal E, et al. Clinical outcome in asymptomatic severe aortic stenosis: insights from the new proposed aortic stenosis grading classification. J Am Coll Cardiol 2012;59:235–43.
7. Marwick TH. Application of 3D echocardiography to everyday practice: development of normal ranges is step 1. J Am Coll Cardiol Img 2012;5:1198–200.
8. Chahal NS, Lim TK, Jain P, Chambers JC, Kooner JS. Senior population-based reference values for 3D echocardiographic LV volumes and ejection fraction. J Am Coll Cardiol Img 2012;5:1191–7.
9. Mor-Avi V, Yodwut C, Jenkins C, et al. Real-time 3D echocardiographic quantification of left atrial volume: multicenter study for validation with CMR. J Am Coll Cardiol Img 2012;5:769–77.
10. Cavalcante JL, Rodriguez LL, Kapadia S, Tuzcu EM, Stewart WJ. Role of echocardiography in percutaneous mitral valve interventions. J Am Coll Cardiol Img 2012;5:733–46.
11. Faletra FF, Pedrazzini G, Pasotti E, Mocceti T. Side-by-side comparison of fluoroscopy, 2D and 3D TEE during percutaneous edge-to-edge mitral valve repair. J Am Coll Cardiol Img 2012;5:656–61.
12. Marwick TH. Measurement of strain and strain rate by echocardiography. J Am Coll Cardiol 2006;47:1313–27.
13. Phelan D, Collier P, Thavendiranathan P, et al. Relative apical sparing of longitudinal strain using two-dimensional speckle-tracking echocardiography is both sensitive and specific for the diagnosis of cardiac amyloidosis. Heart 2012;98:1442–8.
14. Marwick TH, Dilsizian V, Narula J. Ischemic episode and hanging on to a painful memory. J Am Coll Cardiol Img 2012;5:126–8.
15. Ishii K, Imai M, Suyama T, et al. Exercise-induced post-ischemic left ventricular delayed relaxation or diastolic stunning: is it a reliable marker in detecting coronary artery disease? J Am Coll Cardiol 2009;53:698–705.
16. Asanuma T, Fukuta Y, Masuda K, Hioki A, Iwasaki M, Nakatani S. Assessment of myocardial ischemic memory using speckle tracking echocardiography. J Am Coll Cardiol Img 2012;5:1–11.
17. Herrmann S, Stork S, Niemann M, et al. Low-gradient aortic valve stenosis myocardial fibrosis and its influence on function and outcome. J Am Coll Cardiol 2011;58:402–12.
18. La Gerche A, Burns AT, D'Hooge J, Macisaac AI, Heidbuchel H, Prior DL. Exercise strain rate imaging demonstrates normal right ventricular contractile reserve and clarifies ambiguous resting measures in endurance athletes. J Am Soc Echocardiogr 2012;25:253–62.
19. Dave JK, Halldorsdottir VG, Eisenbrey JR, et al. Noninvasive LV-pressure estimation using subharmonic emissions from microbubbles. J Am Coll Cardiol Img 2012;5:87–92.
20. Shaw LJ, Hage FG, Berman DS, Hachamovitch R, Iskandrian A. Prognosis in the era of comparative effectiveness research. Where is nuclear cardiology now and where Should it be? J Nucl Cardiol 2012;19:1026–43.
21. Sheth T, Yusuf S. Enhancing risk prediction with PET coronary flow reserve. J Am Coll Cardiol Img 2012;5:1035–6.
22. Fiechter M, Ghadri JR, Gebhard C, et al. Diagnostic value of 13N-ammonia myocardial perfusion PET: added value of myocardial flow reserve. J Nucl Med 2012;53:1230–4.
23. Murthy VL, Naya M, Foster CR, et al. Association between coronary vascular dysfunction and cardiac mortality in patients with and without diabetes mellitus. Circulation 2012;126:1858–68.
24. Murthy VL, Naya M, Foster CR, et al. Coronary vascular dysfunction and prognosis in patients with chronic kidney disease. J Am Coll Cardiol 2012;5:1025–34.
25. Bucerius J, Manka C, Schmaljohann J, et al. Feasibility of 18F-2-fluoro-A85380-PET imaging of human vascular nicotininc acetylcholine

receptors in vivo. J Am Coll Cardiol Img 2012;5:528–36.

26. Dweck MR, Chow MW, Joshi NV, et al. Coronary arterial 18F-sodium fluoride uptake. J Am Coll Cardiol 2012;59:1539–48.
27. Dweck MR, Jones C, Joshi NV, et al. Assessment of valvular calcification and inflammation by positron emission tomography in patients with aortic stenosis. Circulation 2012;5:76–86.
28. Dilsizian V, Zynda TK, Petrov A, et al. Molecular imaging of human ACE-1 expression in transgenic rats. J Am Coll Cardiol Img 2012; 5:409–18.
29. Fukushima K, Bravo PE, Higuchi T, et al. Molecular hybrid positron emission tomography/computed tomography imaging of cardiac angiotensin II type 1 receptors. J Am Coll Cardiol 2012;60:2527–34.
30. Schindler TH, Dilsizian V. Cardiac positron emission tomography/computed tomography imaging of the renin-angiotensin system in humans holds promise for image-guided approach to heart failure therapy. J Am Coll Cardiol 2012;24:2535–8.
31. Chugh AR, Beache GM, Loughran JH, et al. Administration of cardiac stem cells in patients with ischemic cardiomyopathy: the SCIPIO trial. Surgical aspects and interim analysis of myocardial function and viability by magnetic resonance. Circulation 2012; 126 Suppl:S54–64.
32. Hsu LY, Groves DW, Aletras AH, Kellman P, Arai AE. A quantitative pixel wise measurement of myocardial blood flow by contrast-enhanced first-pass CMR perfusion imaging: microsphere validation in dogs and feasibility study in humans. J Am Coll Cardiol Img 2012;5:154–66.
33. Morton G, Chiribiri A, Ishida M, et al. Quantification of absolute myocardial perfusion in patients with coronary artery disease: comparison between cardiovascular magnetic resonance and positron emission tomography. J Am Coll Cardiol 2012;60:1546–55.
34. Jogya R, Kozerke S, Morton G, et al. Validation of dynamic 3-dimensional whole heart magnetic resonance myocardial perfusion imaging against fractional flow reserve for the detection of significant coronary artery disease. J Am Coll Cardiol 2012;60:756–65.
35. Manka R, Paetsch I, Kozerke S, et al. Whole-heart dynamic three-dimensional magnetic resonance perfusion imaging for the detection of coronary artery disease defined by fractional flow reserve: determination of volumetric myocardial ischaemic burden and coronary lesion location. Eur Heart J 2012; 33:2016–24.
36. Greenwood JP, Maredia N, Younger JF, et al. Cardiovascular magnetic resonance and single-photon emission computed tomography for diagnosis of coronary heart Disease (CE-MARC): a prospective trial. Lancet 2012;379:453–60.
37. Underwood R, Harbinson M, Kelion A, Sabharwal N. CMR versus SPECT for diagnosis of coronary heart disease. Lancet 2012;379:2146.
38. Jaarsma C, Leiner T, Bekkers SC, et al. Diagnostic performance of noninvasive myocardial perfusion imaging using single-photon emission computed tomography, cardiac magnetic resonance, and positron emission tomography for the detection of obstructive coronary artery disease. A meta-analysis. J Am Coll Cardiol 2012;59:1719–28.
39. Schelbert EB, Cao JJ, Sigurdsson S, et al. Prevalence and prognosis of unrecognized myocardial infarction determined by cardiac magnetic resonance in older adults. JAMA 2012; 308:890–7.
40. Kim RJ, Wu E, Rafael A, et al. The use of contrast-enhanced magnetic resonance imaging to identify reversible myocardial dysfunction. N Engl J Med 2000;343:1445–53.
41. Romero J, Xue X, Gonzalez W, Garcia MJ. Imaging assessing viability in patients with chronic left ventricular dysfunction due to coronary artery disease. A meta-analysis of prospective trials. J Am Coll Cardiol Img 2012;5: 494–508.
42. Gerber BL, Rousseau MF, Ahn SA, et al. Prognostic value of myocardial viability by delayed-enhanced magnetic resonance in patients with coronary artery disease and low ejection fraction. J Am Coll Cardiol 2012;59: 825–35.
43. Lurz P, Eitel I, Adam J, et al. Diagnostic performance of CMR imaging compared with EMB in patients with suspected myocarditis. J Am Coll Cardiol Img 2012;5:513–24.
44. Leyva F, Taylor RJ, Foley PW, et al. Left ventricular midwall fibrosis as a predictor of mortality and morbidity after cardiac resynchronization therapy in patients with nonischemic cardiomyopathy. J Am Coll Cardiol 2012; 60:1659–67.
45. Klem I, Weinsaft JW, Bahnson TD, et al. Assessment of myocardial scarring improves risk stratification in patients evaluated for cardiac defibrillator implantation. J Am Coll Cardiol 2012; 60:408–20.
46. Todiere G, Aquaro GD, Piaggi P, et al. Progression of myocardial fibrosis assessed with cardiac magnetic resonance in hypertrophic cardiomyopathy. J Am Coll Cardiol 2012;60:922–9.
47. Green JJ, Berger JS, Kramer CM, Salerno M. Prognostic value of late gadolinium enhancement in clinical outcomes for hypertrophic cardiomyopathy. J Am Coll Cardiol Img 2012; 5:370–7.
48. Rowin EJ, Maron MS, Lesser JR, Maron BJ. CMR with late gadolinium enhancement in genotype positive-phenotype negative hypertrophic cardiomyopathy. J Am Coll Cardiol Img 2012;5:119–22.
49. Grün S, Schumm J, Greulich S, et al. Long-term follow-up of biopsy-proven viral myocarditis: predictors of mortality and incomplete recovery. J Am Coll Cardiol 2012;59:1604–15.
50. Dall'armellina E, Piechnik SK, Ferreira VM, et al. Cardiovascular magnetic resonance by non contrast T1-mapping allows assessment of severity of injury in acute myocardial infarction. J Cardiovasc Magn Reson 2012;14:15.
51. Ugander M, Bagi PS, Oki AJ, et al. Myocardial edema as detected by pre-contrast T1 and T2 CMR delineates area at risk associated with acute myocardial infarction. J Am Coll Cardiol Img 2012;5:596–603.
52. Thavendiranathan P, Walls M, Giri S, et al. Improved detection of myocardial involvement in acute inflammatory cardiomyopathies using T2 mapping. Circ Cardiovasc Imaging 2012;5:102–10.
53. Ferreira VM, Piechnik SK, Dall'armellina E, et al. Non-contrast T1-mapping detects acute myocardial edema with high diagnostic accuracy: a comparison to T2-weighted cardiovascular magnetic resonance. J Cardiovasc Magn Reson 2012;14:42.
54. van Heeswijk RB, Feliciano H, Bongard C, et al. Free-breathing 3 T magnetic resonance T2-mapping of the heart. J Am Coll Cardiol Img 2012;5:1231–9.
55. Eitel I, Thiele H. CMR mapping techniques for myocardium at risk: next step into a bright future? J Am Coll Cardiol Img 2012;5:604–6.
56. Yoon YE, Kitagawa K, Kato S, et al. Prognostic value of coronary magnetic resonance angiography for prediction of cardiac events in patients with suspected coronary artery disease. J Am Coll Cardiol 2012;60:2316–22.
57. Ratnayaka K, Faranesh AZ, Hansen MS, et al. Real-time MRI-guided right heart catheterization in adults using passive catheters. Eur Heart J 2013;34:380–9.

58. Sommer P, Grothoff M, Eitel C, et al. Feasibility of real-time magnetic resonance imaging-guided electrophysiology studies in humans. Europace 2013;15:101–8.
59. Ganesan AN, Selvanayagam JB, Mahajan R, et al. Mapping and ablation of the pulmonary veins and cavotricuspid isthmus with a magnetic resonance imaging-compatible externally irrigated ablation catheter and integrated electrophysiology system. Circ Arrhythm Electrophysiol 2012;5:1136–42.
60. Detrano R, Guerci AD, Carr JJ, et al. Coronary calcium as a predictor of coronary events in four racial or ethnic groups. N Engl J Med 2008;358:1336–45.
61. Okwuosa TM, Greenland P, Ning H, Liu K, Lloyd-Jones DM. Yield of screening for coronary artery calcium in early middle-age adults based on the 10-year Framingham Risk Score: the CARDIA study. J Am Coll Cardiol Img 2012;5:923–30.
62. McEvoy JW, Blaha MJ, Rivera JJ, et al. Mortality rates in smokers and nonsmokers in the presence or absence of coronary artery calcification. J Am Coll Cardiol Img 2012;5:1037–45.
63. Hou ZH, Lu B, Gao Y, et al. Prognostic value of coronary CT angiography and calcium score for major adverse cardiac events in outpatients. J Am Coll Cardiol Img 2012;5:990–9.
64. Yeboah J, McClelland RL, Polonsky TS, et al. Comparison of novel risk markers for improvement in cardiovascular risk assessment in intermediate-risk individuals. JAMA 2012;308:788–95.
65. Litt HI, Gatsonis C, Snyder B, et al. CT Angiography for safe discharge of patients with possible acute coronary syndromes. N Engl J Med 2012;366:1393–403.
66. Hoffmann U, Truong QA, Schoenfeld DA, et al. Coronary CT angiography versus standard evaluation in acute chest pain. N Engl J Med 2012;367:299–308.
67. Otaki Y, Arsanjani R, Gransar H, et al. What have we learned from CONFIRM? Prognostic implications from a prospective multicenter international observational cohort study of consecutive patients undergoing coronary computed tomographic angiography. J Nucl Cardiol 2012;19:787–95.
68. Min JK, Berman DS, Dunning A, et al. All-cause mortality benefit of coronary revascularization vs. medical therapy in patients without known coronary artery disease undergoing coronary computed tomographic angiography: results from CONFIRM (COronary CT Angiography EvaluatioN For Clinical Outcomes: An InteRnational Multicenter Registry). Eur Heart J 2012;33:3088–97.
69. Cho I, Shim J, Chang HJ, et al. Prognostic value of multidetector coronary computed tomography angiography in relation to exercise electrocardiogram in patients with suspected coronary disease. J Am Coll Cardiol 2012;21:2205–15.
70. Cho I, Chang HJ, Sung JM, et al., CONFIRM Investigators. Coronary computed tomographic angiography and risk of all-cause mortality and nonfatal myocardial infarction in subjects without chest pain syndrome from the CONFIRM Registry (coronary CT angiography evaluation for clinical outcomes: an international multicenter registry). Circulation 2012;126:304–13.
71. Sato A, Nozato T, Hikita H, et al. Prognostic value of myocardial contrast delayed enhancement with 64-slice multidetector computed tomography after acute myocardial infarction. J Am Coll Cardiol 2012;59:730–8.
72. George RT, Arbab-Zadeh A, Miller JM, et al. Computed tomography myocardial perfusion imaging with 320-row detector computed tomography accurately detects myocardial ischemia in patients with obstructive coronary artery disease. Circ Cardiovasc Imaging 2012;5:333–40.
73. Ko BS, Cameron JD, Leung M, et al. Combined CT coronary angiography and stress myocardial perfusion imaging for hemodynamically significant stenosis in patients with suspected coronary artery disease. A comparison with fractional flow reserve. J Am Coll Cardiol Img 2012;5:1097–111.
74. Yoon YE, Choi JH, Kim JH, et al. Noninvasive diagnosis of ischemia-causing coronary stenosis using CT angiography: diagnostic value of transluminal attenuation gradient and fractional flow reserve computed from coronary CT angiography compared to invasively measured fractional flow reserve. J Am Coll Cardiol Img 2012;5:1088–96.
75. Choi JH, Min JK, Labounty TM, et al. Intracoronary transluminal attenuation gradient in coronary CT angiography for determining coronary artery stenosis. J Am Coll Cardiol Img 2011;4:1149–57.
76. Koo BK, Erglis A, Doh JH, et al. Diagnosis of ischemia-causing coronary stenoses by noninvasive fractional flow reserve computed from coronary computed tomographic angiograms. Results from the prospective multicenter DISCOVER-FLOW (Diagnosis of Ischemia-Causing Stenoses Obtained Via Noninvasive Fractional Flow Reserve) study. J Am Coll Cardiol 2011;58:1989–97.
77. Min JK, Leipsic J, Pencina MJ, et al. Diagnostic accuracy of fractional flow reserve from anatomic CT angiography. JAMA 2012;308:1237–45.
78. Cho I, Shim J, Chang HJ, et al. Prognostic value of multidetector coronary computed tomography angiography in relation to exercise electrocardiogram in patients with suspected coronary artery disease. J Am Coll Cardiol 2012;60:2205–15.
79. de Azevedo CF, Hadlich MS, Bezerra SG, et al. Prognostic value of CT angiography in patients with inconclusive functional stress tests. J Am Coll Cardiol Img 2011;4:740–51.
80. Andreini D, Pontone G, Mushtaq S, et al. A long-term prognostic value of coronary CT angiography in suspected coronary artery disease. J Am Coll Cardiol Img 2012;5:690–701.
81. Motoyama S, Sarai M, Harigaya H, et al. Computed tomographic angiography characteristics of atherosclerotic plaques subsequently resulting in acute coronary syndrome. J Am Coll Cardiol 2009;54:49–57.
82. Maurovich-Horvat P, Schlett CL, Alkadhi H, et al. The napkin ring sign indicates advanced atherosclerotic lesions in coronary CT angiography. J Am Coll Cardiol Img 2012;5:1243–52.
83. Watabe H, Sato A, Akiyama D, et al. Impact of coronary plaque composition on cardiac troponin elevation after percutaneous coronary intervention in stable angina pectoris. A computed tomography analysis. J Am Coll Cardiol 2012;59:1881–8.
84. Achenbach S, Delgado V, Hausleiter J, Schoenhagen P, Min JK, Leipsic JA. SCCT expert consensus document on computed tomography imaging before transcatheter aortic valve implantation (TAVI)/transcatheter aortic valve replacement (TAVR). J Cardiovasc Comput Tomogr 2012;6:366–80.
85. Bloomfield GS, Gillam LD, Hahn RT, et al. A practical guide to multimodality imaging of transcatheter aortic valve replacement. J Am Coll Cardiol Img 2012;5:441–55.
86. Yared K, Garcia-Camarero T, Fernandez-Friera L, et al. Impact of aortic regurgitation after transcatheter aortic valve implantation: results from the REVIVAL trial. J Am Coll Cardiol Img 2012;5:469–77.

87. Jilaihawi H, Kashif M, Fontana G, et al. Cross-sectional computed tomographic assessment improves accuracy of aortic annular sizing for transcatheter aortic valve replacement and reduces the incidence of paravalvular aortic regurgitation. J Am Coll Cardiol 2012;59:1275–86.
88. Hayashida K, Bouvier E, Lefèvre T, et al. Impact of CT-guided valve sizing on post-procedural aortic regurgitation in transcatheter aortic valve implantation. Impact of CT-guided valve sizing on post-procedural aortic regurgitation in transcatheter aortic valve implantation. EuroIntervention 2012;8:546–55.
89. Arnold M, Achenbach S, Pfeiffer I, et al. A method to determine suitable fluoroscopic projections for transcatheter aortic valve implantation by computed tomography. J Cardiovasc Comput Tomogr 2012;6:422–8.
90. Binder RK, Leipsic J, Wood D, et al. Prediction of optimal deployment projection for transcatheter aortic valve replacement: angiographic 3-dimensional reconstruction of the aortic root versus multidetector computed tomography. Circ Cardiovasc Interv 2012;5:247–52.

Key Words: cardiac computed tomography ■ cardiac magnetic resonance ■ contrast ■ coronary angiography ■ echocardiography ■ late gadolinium enhancement ■ PET ■ SPECT ■ strain ■ strain rate.